Discrete-Ordinates and Finite-Volume Methods for Radiation Heat Transfer

J. C. Chai
School of Mechanical and Aerospace Engineering
Nanyang Technological University
Singapore-639798
Email-mckchai@ntu.edu.sg

P. Rath
School of Mechanical and Aerospace Engineering
Nanyang Technological University
Singapore-639798
Email-pe1756649@ntu.edu.sg

Abstract

This article presents Discrete Ordinate and Finite Volume methods for modeling radiation heat transfer processes. In order to provide a *focus* to this article, only the Finite Volume method is described in detail. The discrete-ordinates method and its variants are discussed where it is needed. A detailed formulation of the radiative transport problem using the finite volume method is presented. The solution methodology using the Finite Volume method is briefly described.

Nomenclature

a	coefficient of the discretization equation
A	area of control volume faces
b	source term in the discretization equation
D_c^l	direction cosine integrated over $\Delta\Omega^l$
$\hat{e}_x, \hat{e}_y, \hat{e}_z$	unit vectors in x, y, and z directions
I	intensity
L	number of control angles
$\hat{n}$	unit outward normal vector
s	distance traveled by a beam
S	source function
t	time
x, y, z	coordinate directions
β	extinction coefficient
ΔV	volume of control volume
$\Delta\Omega^l$	control angle
ε	wall emissivity
κ	absorption coefficient
μ, ξ	direction cosines in x, y directions
α, γ	mass flow rate per unit area (Eq. 10)
ρ	density or wall reflectivity
θ	polar angle measured from $\hat{e}_z$
σ	Stefan-Boltzmann constant or scattering coefficient
ϕ	azimuthal angle measured from $\hat{e}_x$ or general dependent variable
w	angular weight
Φ	scattering phase function

Subscripts

b	blackbody

E, W, N, S	east, west, north, and south neighbors of P
e, w, n, s	east, west, north, and south control-volume faces
P	control volume P
x, *y*, *z*	coordinate directions

Superscripts

l, l'	angular directions

1 Introduction

The number of publications on radiation heat transfer procedures has increased rapidly over the past few years. As a result, a comprehensive review of all literature dealing with the subject will not be attempted here. In order to provide a *focus* to this article, only the Finite Volume (FV) method is described in detail. The discrete-ordinates (DO) method and its variants will be discussed when their inclusion is needed.

As mentioned earlier, this article focuses on the method of solution rather than on the different physical models. As a result, nongray models, which are very important for a variety of applications, are not discussed here. Combined mode heat transfer (combined diffusion, convection and radiation) is also not considered in this article.

This article focuses on presenting a numerical method for radiative heat transfer processes. It is based on the finite-volume (FV) method [14, 20, 33]. The main elements of the calculation procedure were presented by Chai and co-workers [20, 24, 25, 46, 55, 57]. This article presents much of the same material in a condensed form. Readers are referred to Chai and Patankar [46], Siegel and Howell [48], and Modest [53], for more thorough collections of articles on the FV and DO methods for radiative transfer.

1.1 Outline of the Article

This chapter is divided into ten sections. The equations governing radiative heat transfer i.e. the transient radiative transfer equation (TRTE), boundary conditions and other related relations are presented in Section 2. Before presenting the FV method for radiation heat transfer, a discussion of the flux, DO and FV methods is given in Section 3. Section 4 shows the discretization of the spatial and angular domains. The TRTE is converted into a set of algebraic equations in Section 5. Other details related to the discretization of the TRTE are also discussed in this section. Spatial differencing schemes are discussed in section 6. Treatment of irregular geometries using FV method is discussed in section 7. Shortcomings of the FV method like the ray effect and the false scattering are discussed in section 8. Some prepresentative works on DO and FV methods are presented in section 9 followed by some concluding remarks given in section 10.

2 Governing Equations and Related Quantities

The equations governing the "transport" of radiant energy, boundary conditions, scattering phase function and other related quantities are presented in this section.

2.1 Transient Radiative Transfer Equation

The TRTE for a gray medium can be written as

$$\frac{\partial I(\vec{r},\hat{s},t)}{\partial t}+\frac{\partial I(\vec{r},\hat{s},t)}{\partial s}=-\beta(\vec{r})I(\vec{r},\hat{s},t)+\kappa(\vec{r})I_b(\vec{r},t)+\frac{\sigma(\vec{r})}{4\pi}\int_{4\pi} I(\vec{r},\hat{s}',t)\Phi(\hat{s}',\hat{s})d\Omega' \tag{1}$$

From Eq. (1), it is clear that radiant intensity I depends on spatial position $\vec{r}$ and angular direction $\hat{s}$. The solution of Eq. (1) requires the specification of the boundary conditions. Although the method described in this chapter can handle non-diffuse and semitransparent surfaces, only opaque diffuse surfaces are described for simplicity.

2.2 Boundary Condition for an Opaque Diffuse Surface

The radiant intensity leaving an opaque diffuse surface contains emitted and reflected energy. This can be written as

$$I(\vec{r},\hat{s},t)=\varepsilon(\vec{r})I_b(\vec{r},t)+\frac{\rho(\vec{r})}{\pi}\int_{\hat{s}'\bullet\hat{n}<0} I(\vec{r},\hat{s}',t)\left|\hat{s}'\bullet\hat{n}\right|d\Omega' \tag{2}$$

Equation (2) provides the boundary intensity for the TRTE.

2.3 Scattering Phase Function

The scattering phase function Φ in the TRTE describes how radiant energy is scattered by a participating medium. Scattering can be classified into two categories. These are isotropic and anisotropic scattering. Isotropic scattering scatters energy equally into all directions. Anisotropic scattering can be further divided into backward and forward scattering. Backward scattering scatters more energy into the backward directions, while forward scattering scatters more energy into the forward directions. Scattering phase functions satisfy

$$\int_{4\pi} \Phi(\hat{s}', \hat{s}) d\Omega' = 4\pi \tag{3}$$

2.4 Radiation Heat Transfer Relations

A few useful quantities are defined in this subsection for ease of reference. The incident radiation is defined as

$$G(\vec{r}, t) = \int_{4\pi} I(\vec{r}, \hat{s}, t) d\Omega \tag{4}$$

The radiative heat flux in direction *i* is defined as

$$q_i(\vec{r}, t) = \int_{2\pi} I(\vec{r}, \hat{s}, t)(\hat{s} \bullet \hat{i}) d\Omega \tag{5}$$

where $\hat{i}$ is the unit vector pointing in the *i* direction. For example, the radiative heat flux in the *x* direction is

$$q_x(\vec{r}, t) = \int_{2\pi} I(\vec{r}, \hat{s}, t)(\hat{s} \bullet \hat{e}_x) d\Omega \tag{6}$$

The divergence of the radiative heat flux is

$$\nabla \bullet q = \kappa[4\pi I_b(\vec{r}, t) - G(\vec{r}, t)] \tag{7}$$

Equation (7) defines an important quantity in combined mode heat transfer as well as in radiation-dominated processes. In the absence of a heat source/sink, a system is in radiative equilibrium if other modes of heat transfer are absent. Under such condition, $\nabla \bullet q = 0$, and the temperature of the medium can be obtained from Eq. (7). In combined mode heat transfer processes with a participating medium, $\nabla \bullet q$ is the radiation source term in the energy equation.

3 THE FLUX, DISCRETE-ORDINATES AND FINITE-VOLUME METHODS

A brief overview of the flux, DO and FV methods is given in this section. Since radiant intensities have to be resolved in both the angular and spatial domains, a complete discretization procedure should show these two discretizations. However, the main difference in the flux, DO and FV methods lies in the treatment of the *angular* space. Therefore, this section focuses on the discretization of the *angular* space. Spatial discretization practices will be discussed in a later section. A detailed evaluation of the relations among the three methods is given at the end of this section.

3.1 The Flux Method

The flux method, also known as the Schuster-Schwarzschild approximation, was proposed by Schuster [1] and Schwarzschild [2] for one-dimensional radiative transfer. The actual intensities (Fig. 1a) are approximated by dividing the 4π solid angle into two solid angles (one in each coordinate direction). The magnitude of the radiative intensity over the positive coordinate direction is assumed uniform. The magnitude of the radiant intensity in the negative coordinate direction is also assumed to be uniform but is allowed to be different from the magnitude of the intensity in the positive coordinate direction. Radiant energy is allowed to travel in *all* directions within the positive and negative coordinate directions. This approximation is depicted in Fig. 1b and can be written as

$$I = \begin{cases} I^+ & \hat{n}_z \bullet \hat{s} > 0 \quad \text{positive coordinate direction} \\ I^- & \hat{n}_z \bullet \hat{s} < 0 \quad \text{negative coordinate direction} \end{cases} \tag{8}$$

For isotropic scattering (Φ = 1), the Radiative Transfer Equation (RTE) for the positive coordinate direction can be written as

$$\frac{dI^+}{dz} = -\beta I^+ + \kappa I_b + \frac{\sigma}{4\pi}\left(I^+ + I^-\right) \tag{9}$$

Integrating Eq. (9) over the positive coordinate hemisphere gives

$$\frac{dI^+}{dz}\int_{\hat{n}_z\bullet\hat{s}>0}(\hat{n}_z\bullet\hat{s})d\Omega=\left[-\beta I^+ +\kappa I_b+\frac{\sigma}{2}\left(I^+ +I^-\right)\right]\int_{\hat{n}_z\bullet\hat{s}>0}d\Omega \tag{10a}$$

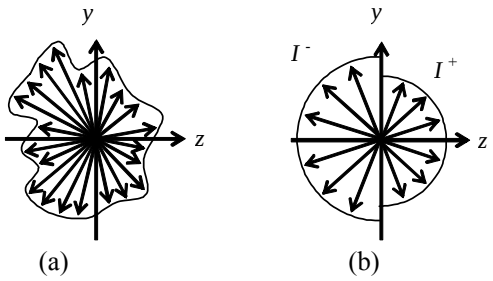

Figure 1 Radiant intensity distribution: (a) actual intensity, (b) two-flux method.

or

$$\frac{1}{2}\frac{dI^+}{dz}=-\beta I^+ +\kappa I_b+\frac{\sigma}{2}\left(I^+ +I^-\right) \tag{10b}$$

A similar equation for the negative coordinate direction can be written as

$$\frac{1}{2}\frac{dI^-}{dz}=-\beta I^- +\kappa I_b+\frac{\sigma}{2}\left(I^+ +I^-\right) \tag{10c}$$

In summary, the two-flux method divides the *angular* space into two solid angles (one in each coordinate direction) in which the *magnitudes* of the radiant intensities are assumed constant. Radiation is allowed to travel in *all* directions within each solid angle (see Fig. 1b). This approach reduces the RTE to two ordinary differential equations, which can be solved using any convenient method. If the spatial domain is discretized into a finite number of control volumes, a discretization equation can be formulated for each control volume, and appropriate solution procedures can be employed to solve the resulting set of algebraic equations.

3.2 The Discrete-Ordinates Method

Most solution procedures for radiation heat transfer, including the DO method, were developed for astrophysics and neutron transport applications. Khalil and Truelove [6] and Fiveland [8-10] adopted the DO method to model radiative heat transfer processes and reported DO solutions for radiation heat transfer problems. Over the past few years, there has been a tremendous increase in the number of papers on the modeling of radiation heat transfer using the DO method. Due to its popularity, it is appropriate to examine the DO method and compare it with the flux and FV methods.

Chandrasekhar [3] proposed the DO method in 1960. It was realized that the two-flux method could not accurately model anisotropic scattering with the two-solid-angle discretization practice. In the DO approximation, the actual radiation field (Fig. 2a) is divided into a finite number of discrete directions (Fig. 2b). The RTE at a *discrete* direction for one-dimensional problems can be written as

$$\mu^l\frac{dI^l}{dz}=-\beta I^l+\kappa I_b+\frac{\sigma}{4\pi}\sum_{l'=1}^{L}I^{l'}\overline{\Phi}^{l'l}w^{l'} \tag{11}$$

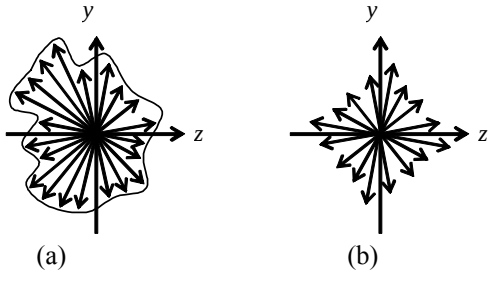

Figure 2 Radiant intensity distribution: (a) actual intensity, (b) DO method.

For nonscattering media in a black enclosure, radiant intensity along any direction can be calculated directly from Eq. (11) *without* solid-angle reference. These angular directions can, in principle, be chosen arbitrarily. However, several procedures have been developed to generate quadrature sets (ordinate directions and angular weights) that integrate the radiant energy and inscattering terms accurately. Therefore, exact locations of these angular directions are chosen such that the products of the angular directions and their weights satisfy certain full-range and half-range moment constraints.

The full-range moments are also important if the scattering phase function in the RTE is to be evaluated correctly. Since most quadrature sets do not integrate the scattering phase function correctly, phase functions are normalized to ensure that Eq. (3) is satisfied. This normalization can be written as

$$\frac{1}{4\pi}\sum_{l'=1}^{L}\Phi^{l'l}w^{l'}=1 \tag{12}$$

This problem is avoided in the FV method.

3.3 The Finite-Volume Method

The FV method for radiation heat transfer presented in the literature has formulated the discretization equation by integration over both spatial control volume and angular control (solid) angle. For the purpose of this discussion, spatial and temporal discretization is deferred and only angular discretization is considered. A typical control (solid) angle is shown in Fig. 3.

Integrating the RTE over a control angle (Fig. 3) gives

$$\int_{\Delta\Omega^l}\frac{dI}{ds}d\Omega=\int_{\Delta\Omega^l}\left(-\beta I+\kappa I_b\right)d\Omega+\frac{\sigma}{4\pi}\int_{\Delta\Omega^l}\int_{4\pi}\left(I'\Phi\right)d\Omega' d\Omega \tag{13}$$

For a one-dimensional problem, the left side of Eq. (13) can be written as

$$\int_{\Delta\Omega^l}\frac{dI}{dz}\left(\hat{n}_z\bullet\hat{s}\right)d\Omega=\int_{\Delta\Omega^l}\left(-\beta I+\kappa I_b\right)d\Omega+\frac{\sigma}{4\pi}\int_{\Delta\Omega^l}\int_{4\pi}\left(I'\Phi\right)d\Omega' d\Omega \tag{14}$$

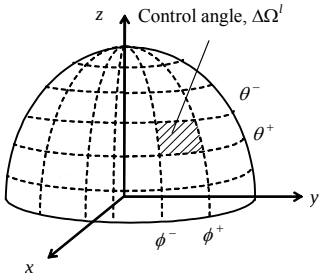

Figure 3 Control (solid) angle for the FV method.

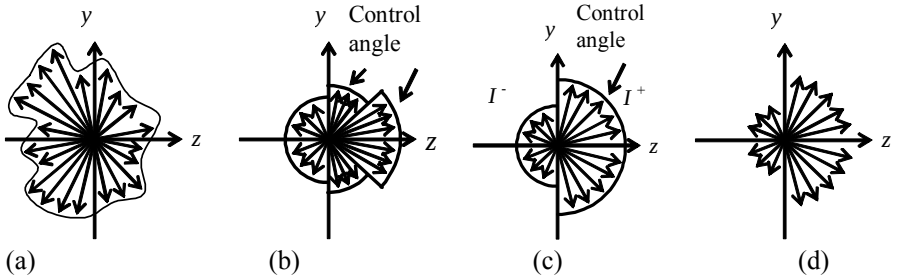

Figure 4 Radiant intensity distribution: (a) actual intensity, (b) FV method, (c) two-control-angle FV discretization, (d) discrete direction discretization.

In the control volume approach, the intensity is assumed constant within a control angle (Fig. 4b). Equation (14) can be simplified to

$$\frac{dI}{dz} D_{cz}^{l} = \left(-\beta I + \kappa I_b\right)\Delta\Omega^{l} + \frac{\sigma}{4\pi}\Delta\Omega^{l}\int_{4\pi}\left(I'\Phi\right)d\Omega' \tag{15}$$

where

$$D_{cz}^{l} = \int_{\Delta\Omega^{l}}\left(\hat{n}_z \bullet \hat{s}\right)d\Omega \qquad\qquad \Delta\Omega^{l} = \int_{\Delta\Omega^{l}} d\Omega \tag{16}$$

When two control angles (one in each coordinate direction), as shown in Fig. 4c, are used to discretize the angular space in an isotropically scattering medium, Eq. (15) becomes

$$\frac{1}{2}\frac{dI^{+}}{dz} = -\beta I^{+} + \kappa I_b + \frac{\sigma}{2}\left(I^{+} + I^{-}\right) \tag{17a}$$

$$\frac{1}{2}\frac{dI^{-}}{dz} = -\beta I^{-} + \kappa I_b + \frac{\sigma}{2}\left(I^{+} + I^{-}\right) \tag{17b}$$

These two equations are *identical* to the equations obtained by the two-flux method.

For an isotropically scattering medium, if radiant energy is allowed to travel along *discrete* directions as shown in Fig. 4d, Eq. (14) can be simplified to

$$\frac{dI^{l}}{dz}\mu^{l}\int_{\Delta\Omega^{l}} d\Omega = \left(-\beta I^{l} + \kappa I_b\right)\int_{\Delta\Omega^{l}} d\Omega + \frac{\sigma}{4\pi}\int_{4\pi} I'd\Omega'\int_{\Delta\Omega^{l}} d\Omega \tag{18}$$

or

$$\mu^{l}\frac{dI^{l}}{dz} = -\beta I^{l} + \kappa I_b + \frac{\sigma}{4\pi}\sum_{l'=1}^{L} I^{l'}w^{l'} \tag{19}$$

which is the RTE for the DO method (Eq. 11). When a quadrature set that satisfies the half-range first moment is used, Eq. (19) reduces *mathematically* to the two-flux equation.

3.4 Closure

From the above discussion, for one-dimensional problems, the FV method is a higher-order flux method. The discretization equation is formulated by integrating the RTE over a discrete solid angle. In both the two-flux and FV methods, the magnitude of the radiant intensity is assumed uniform over a control angle. Radiation is allowed to travel in *all* directions within a solid angle. When two control angles (one in each coordinate direction) are used, the FV method *always* reduces to the two-flux method.

In multi-dimensional problems, the philosophy of the FV method is slightly different from the philosophy of the four-flux or six-flux methods. The FV method *usually* does not divide the angular space along the four or six coordinate directions as in the flux method. However, the angular discretization practice employed by the four-flux or six-flux methods can of course be accommodated by the FV method.

In the DO method, radiant energy is allowed to travel along *discrete* directions [3]. There is no solid angle integration. For non-scattering media in a black environment, radiant intensity along any direction can be calculated directly without solid angle reference. These angular directions can, in principle, be chosen arbitrarily. However, several procedures have been developed to generate quadrature sets (ordinate directions and angular weights) that integrate the radiant energy and inscattering terms accurately. When a S_2 quadrature set which satisfied the half-range first moment is used in one-dimensional problems, the resulting RTE is *mathematically* similar to that of the two-flux and the FV (with two control angles) methods. However, these equations are obtained using very different principles. The RTE for the DO method can be obtained from the FV method if the radiant energy is restricted to travel along *discrete* directions.

4 DOMAIN DISCRETIZATION

The numerical method described here is based on the control volume approach. Discretization equations are formulated by integrating the RTE over control volumes and control (solid) angles. Control volumes and control angles are subdivisions of the spatial and angular spaces respectively. The next subsections describe these subdivisions.

4.1 Control Volumes and Grid Points

For ease of discussion, a two-dimensional spatial domain is used in this section. Figure 5a shows a structured grid for a rectangular domain. Figure 5b shows an unstructured grid for the same geometry. The term unstructured is used here

to refer to computational grids without any structured order in the *x*- and *y*-directions. It is understood that with proper indexing, an unstructured grid procedure can be used on the grid shown in Fig. 5a.

The control volume boundaries (dashed lines) are drawn first. Grid points are then placed at the geometric centers of the control volumes. Control volume faces should be designed to capture "discontinuities" (see shaded regions of Figs. 5a and 5b) in physical properties, boundary conditions and sources.

4.2 Control Angles

Similar to the spatial discretization, the angular space is discretized by placing control (solid) angle boundaries throughout the 4π solid angle. Although unstructured control angles can be used with the FV method, only structured control angles are discussed in this chapter.

Figure 6a shows a possible angular discretization. The simplest angular discretization is to divide the angular space into N_θ x N_ϕ control angles with equally spaced $\Delta\theta$ and $\Delta\phi$. The size of these control angles can be adjusted to capture the physics of the problem at hand. For example, collimated incidence can be captured by designing a control angle with small $\Delta\theta$ and $\Delta\phi$. Figure 6b shows how collimated incidence can be captured using the present method.

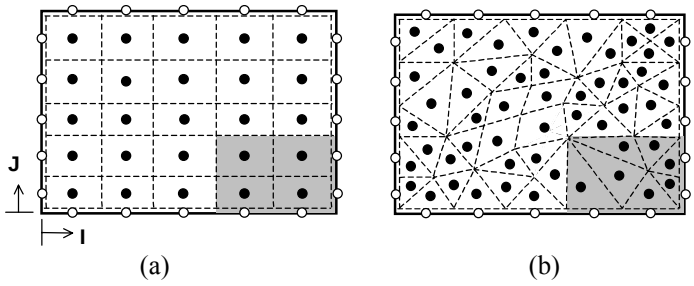

Figure 5 Spatial grids: (a) structured grid, (b) unstructured grid.

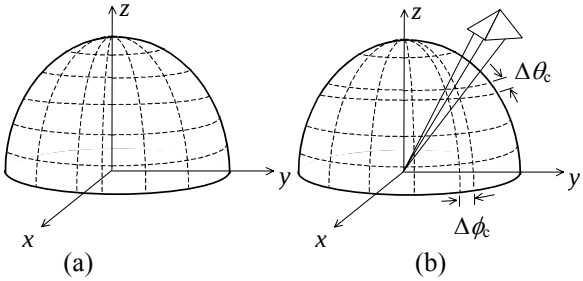

Figure 6 Angular grids: (a) typical, (b) collimated beam.

5 DERIVATION OF THE DISCRETIZATION EQUATION

The discretization equation is the counterpart of the general differential equation (Eq. 1). It is obtained by integrating the TRTE over a typical control volume (Fig. 7a), a control angle (Fig. 7b) and a differential time. Before proceeding with the formulation of the discretization equation, it is important to examine the various possibilities in the definition of the angular direction $\hat{s}$.

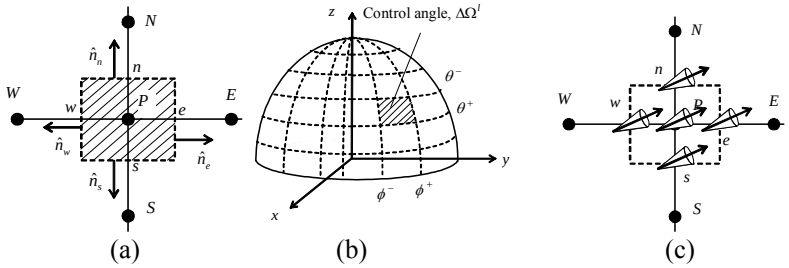

Figure 7 Typical (a) control volume, (b) control angle, (c) control angle orientation.

5.1 Angular Direction

A radiation direction is defined using a set of base vectors. There are at least three common alternatives. These are (1) Cartesian base vectors, (2) cylindrical base vectors, and (3) spherical base vectors. When Cartesian spatial grids are used, the choice of base vectors is obvious. However, when *non*-Cartesian spatial grids are encountered, cylindrical base vectors are the natural choice for cylindrical spatial grids. Similarly, spherical base vectors are the choice for spherical spatial grids. It should be pointed out that the orientation of the Cartesian base vectors does not change with spatial location; thus, a set of fixed values for (θ, ϕ) defines the *same* direction at any spatial location. The orientation of the cylindrical and spherical base vectors changes with the spatial location. Since the TRTE describes the change in radiant intensity along a *straight-line* path, an additional term called the angular redistribution term appears when non-Cartesian base vectors are used. Moder et al. [25] presented a detailed discussion of the angular redistribution term.

Since the purpose of this chapter is to present a procedure which is applicable to *all* spatial grid systems (including non-orthogonal and unstructured grid systems), the radiation direction is defined using the *Cartesian* base vectors. Therefore, the angular direction (Fig. 8) can be described by the unit vector

$$\hat{s} = (\sin\theta\cos\phi)\hat{e}_x + (\sin\theta\sin\phi)\hat{e}_y + (\cos\theta)\hat{e}_z \tag{20}$$

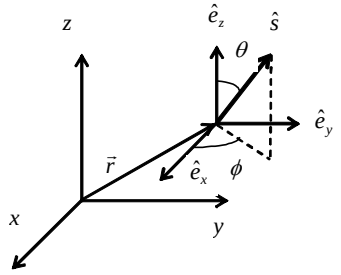

Figure 8 A typical angular direction.

Although this choice eliminates the angular redistribution term in the TRTE, control angle overlap (also called control angle overhang [25]) can appear when non-Cartesian grids are used.

5.2 Linearized Transient Radiative Transfer Equation

In the FV method, the magnitude of the intensity is assumed constant over a control angle. For control angle l, the right side of Eq. (1) can be written as

$$-\beta I^l + \kappa I_b + \frac{\sigma}{4\pi}\int_{4\pi} I^{l'}\,\Phi\,d\Omega^{l'} = -\beta I^l + \kappa I_b + \frac{\sigma}{4\pi}\sum_{l'=1}^{L} I^{l'}\overline{\Phi}^{l'l}\Delta\Omega^{l'}$$

$$= -\left(\beta - \frac{\sigma}{4\pi}\overline{\Phi}^{ll}\Delta\Omega^l\right)I^l + \kappa I_b + \frac{\sigma}{4\pi}\sum_{\substack{l'=1\\ l'\neq l}}^{L} I^{l'}\overline{\Phi}^{l'l}\Delta\Omega^{l'} \tag{21}$$

where $I^l \equiv I(\vec{r},\hat{s},t)$. The *in*-scattering term is summed over all the control angles used to discretized the angular domain, L. In Eq. (21), $\overline{\Phi}^{l'l}$ is the *average* scattering phase function from control angle l' to control angle l to be discussed later. A modified extinction coefficient β_m^l and a modified source function S_m^l can be written as [21]

$$\beta_m^l \equiv \beta - \frac{\sigma}{4\pi}\overline{\Phi}^{ll}\Delta\Omega^l \tag{22}$$

$$S_m^l \equiv \kappa I_b + \frac{\sigma}{4\pi}\sum_{\substack{l'=1\\ l'\neq l}}^{L} I^{l'}\overline{\Phi}^{l'l}\Delta\Omega^{l'} \tag{23}$$

Using these variables, a *linearized* TRTE can be written as

$$\frac{1}{c}\frac{\partial I^l}{\partial t} + \frac{\partial I^l}{\partial s} = -\beta_m^l I^l + S_m^l \tag{24}$$

In scattering media, two observations can be drawn from Eqs. (22)−(24). First, the modified source function no longer contains the intensity of interest, I^l. This reduces the magnitude of the source function. Since the source function is

obtained using the values from the previous iterations, this treatment reduces the dependence of the current iteration on the previous iteration. Second, the modified extinction coefficient scales the optical thickness of a problem and leads to a reduced effective optical thickness.

5.3 Mathematical Formulation

This section presents the formulation of the discretized form of the linearized TRTE (Eq. 24). Integrating Eq. (24) over a typical control volume (Fig. 7a), a typical control angle (Fig. 7b) and a chosen time step gives

$$\int_{\Delta\Omega^l}\int_{\Delta V}\int_{\Delta t}\frac{1}{c}\frac{\partial I^l}{\partial t}dtdVd\Omega+\int_{\Delta t}\int_{\Delta\Omega^l}\int_{\Delta V}\frac{\partial I^l}{\partial s}dVd\Omega dt=\int_{\Delta t}\int_{\Delta\Omega^l}\int_{\Delta V}\left(-\beta_m^l I^l+S_m^l\right)dVd\Omega dt \tag{25}$$

Applying the divergence theorem to the second term of Eq. (25), the following can be written

$$\int_{\Delta\Omega^l}\int_{\Delta V}\int_{\Delta t}\frac{1}{c}\frac{\partial I^l}{\partial t}dtdVd\Omega+\int_{\Delta t}\int_{\Delta\Omega^l}\int_{\Delta A}I^l\left(\hat{s}^l\cdot\hat{n}\right)dAd\Omega dt=\int_{\Delta t}\int_{\Delta\Omega^l}\int_{\Delta V}\left(-\beta_m^l I^l+S_m^l\right)dVd\Omega dt \tag{26}$$

In Eq. (26), $\hat{n}$ is the unit *outward* normal vector shown in Fig. 7a. Physically, the first term of Eq. (26) accounts for the changes of the radiant intensities with time. The second term of Eq. (26) denotes the "inflow" and "outflow" of radiant energy across the control volume faces. The last term represents the attenuation and augmentation of energy within a control volume and control angle.

Following the FV practice, the magnitude of the intensity is assumed constant over a control volume and a control angle. The unsteady term of Eq. (26) can then be written as

$$\int_{\Delta\Omega^l}\int_{\Delta V}\int_{\Delta t}\frac{1}{c}\frac{\partial I^l}{\partial t}dtdVd\Omega=\frac{1}{c}\left(I_P^l-I_P^{l,0}\right)\Delta V\Delta\Omega^l \tag{27}$$

In Eq. (27), $I_P^{l,0}$, and I_P^l are the nodal intensities at the start and at the end of the time step respectively. In the evaluation of the remaining terms of Eq. (26), the choice of the intensities is not apparent. When the fully implicit scheme is used, the remaining terms of Eq. (26) can be written as

$$\int_{\Delta t}\int_{\Delta\Omega^l}\int_{\Delta A}I^l\left(\hat{s}^l\cdot\hat{n}\right)dAd\Omega dt=\sum_i I_i^l A_i\Delta t\int_{\Delta\Omega^l}\left(\hat{s}^l\cdot\hat{n}_i\right)d\Omega^l \tag{28a}$$

$$\int_{\Delta t}\int_{\Delta\Omega^l}\int_{\Delta V}\left(-\beta_m^l I^l+S_m^l\right)dVd\Omega dt=\left(-\beta_{m,P}^l I_P^l+S_{m,P}^l\right)\Delta V\Delta\Omega^l\Delta t \tag{28b}$$

In Eq. (28a), the summation is performed over all control volume boundaries (or interfaces) and I_i^l is the intensity at the interface of interest. Combining Eqs. (27) and (28) gives

$$\frac{1}{c}\left(I_P^l-I_P^{l,0}\right)\Delta V\Delta\Omega^l+\sum_i I_i^l A_i\Delta t\int_{\Delta\Omega^l}\left(\hat{s}^l\cdot\hat{n}_i\right)d\Omega^l=\left(-\beta_{m,P}^l I_P^l+S_{m,P}^l\right)\Delta V\Delta\Omega^l\Delta t \tag{29}$$

For the control volume and control angle orientation shown in Fig. 7c, Eq. (29) can be written as

$$\frac{\Delta V\Delta\Omega^l}{c\Delta t}\left(I_P^l-I_P^{l,0}\right)+A_e D_{ce}^l I_e^l+A_w D_{cw}^l I_w^l+A_n D_{cn}^l I_n^l+A_s D_{cs}^l I_s^l=\left(-\beta_{m,P}^l I_P^l+S_{m,P}^l\right)\Delta V\Delta\Omega^l \tag{30}$$

where

$$D_{ce}^l=\int_{\Delta\Omega^l}\left(\hat{s}^l\cdot\hat{e}_x\right)d\Omega=-D_{cw}^l \tag{31a}$$

$$D_{cn}^l=\int_{\Delta\Omega^l}\left(\hat{s}^l\cdot\hat{e}_y\right)d\Omega=-D_{cs}^l \tag{31b}$$

$$\Delta\Omega^l=\int_{\Delta\Omega^l}d\Omega \tag{31c}$$

$$\beta_{m,P}^l=\beta_P-\frac{\sigma_P}{4\pi}\overline{\Phi}^{ll}\Delta\Omega^l \tag{31d}$$

$$S_{m,P}^{l} = \kappa_P I_{b,P} + \frac{\sigma_P}{4\pi} \sum_{\substack{l'=1 \\ l' \neq l}}^{L} I_P^{l'} \overline{\Phi}^{l'l} \Delta\Omega^{l'} \tag{31e}$$

The areas A_e and A_w (also A_n and A_s) are equal for *Cartesian* coordinates. Separate symbols are used for generality. A spatial differencing scheme is needed to relate the boundary intensities to the nodal intensities. One such scheme is the step or "upwind" scheme that sets the boundary intensities to the "upstream" nodal intensities. For the situation shown in Fig. 7c, Eq. (30) becomes

$$\frac{\Delta V \Delta\Omega^{l}}{c\Delta t}\left(I_P^{l} - I_P^{l,0}\right) + A_e D_{ce}^{l} I_P^{l} + A_w D_{cw}^{l} I_W^{l} + A_n D_{cn}^{l} I_P^{l} + A_s D_{cs}^{l} I_S^{l} = \left(-\beta_{m,P}^{l} I_P^{l} + S_{m,P}^{l}\right) \Delta V \Delta\Omega^{l} \tag{32}$$

Equation (32) can be written as

$$a_P^{l} I_P^{l} = a_W^{l} I_W^{l} + a_S^{l} I_S^{l} + b^{l} \tag{33}$$

where

$$a_W^{l} = A_w \left| D_{cw}^{l} \right|, \qquad a_S^{l} = A_s \left| D_{cs}^{l} \right| \tag{34a}$$

$$a_P^{l} = A_e D_{ce}^{l} + A_n D_{cn}^{l} + \beta_{m,P}^{l} \Delta V \Delta\Omega^{l} + \frac{\Delta V \Delta\Omega^{l}}{c\Delta t} \tag{34b}$$

$$b^{l} = S_{m,P}^{l} \Delta V \Delta\Omega^{l} + \frac{\Delta V \Delta\Omega^{l}}{c\Delta t} I_P^{l,0} \tag{34c}$$

A more compact form of the discretization equation suitable for control angles pointing in all directions can be written as

$$a_P^{l} I_P^{l} = a_W^{l} I_W^{l} + a_E^{l} I_E^{l} + a_S^{l} I_S^{l} + a_N^{l} I_N^{l} + b^{l} \tag{35}$$

where

$$a_E^{l} = \max\left(-A_e D_{ce}^{l}, 0\right), \qquad a_W^{l} = \max\left(-A_w D_{cw}^{l}, 0\right) \tag{36a}$$

$$a_N^{l} = \max\left(-A_n D_{cn}^{l}, 0\right), \qquad a_S^{l} = \max\left(-A_s D_{cs}^{l}, 0\right) \tag{36b}$$

$$\begin{aligned} a_P^{l} = {} & \max\left(A_e D_{ce}^{l}, 0\right) + \max\left(A_w D_{cw}^{l}, 0\right) + \max\left(A_n D_{cn}^{l}, 0\right) + \max\left(A_s D_{cs}^{l}, 0\right) \\ & + \beta_{m,P}^{l} \Delta V \Delta\Omega^{l} + \frac{\Delta V \Delta\Omega^{l}}{c\Delta t} + S_{p,HR}^{l} \end{aligned} \tag{36c}$$

$$b^{l} = S_{m,P}^{l} \Delta V \Delta\Omega^{l} + \frac{\Delta V \Delta\Omega^{l}}{c\Delta t} I_P^{l,0} + S_{c,HR}^{l} \tag{36d}$$

where $S_{c,HR}^{l}$ and $S_{p,HR}^{l}$ are additional sources due to high-resolution spatial differencing schemes [33]. Other quantities are already defined in Eq. (31) and are not repeated here.

5.4 Scattering Phase Function

As mentioned in Section 2.3, the scattering phase function Φ must satisfy

$$\int_{4\pi} \Phi\left(\hat{s}', \hat{s}\right) d\Omega' = 4\pi \tag{37}$$

When a phase function is known analytically, Eq. (37) can be evaluated analytically and satisfied exactly. The average phase function can then be calculated using

$$\overline{\Phi}^{l'l} = \frac{\int_{\Delta\Omega^{l'}} \Phi\left(\hat{s}', \hat{s}\right) d\Omega'}{\Delta\Omega^{l'}} \tag{38}$$

For complicated scattering phase functions, analytic evaluation of Eq. (37) can be computationally intensive or impossible. Although it is possible that the exact evaluation of $\int \Phi\left(\hat{s}', \hat{s}\right) d\Omega'$ might not be possible for certain scattering

phase functions, the value of $\Phi^{l'l}$, which is the scattering from a discrete radiant direction $\hat{s}'$ into $\hat{s}$, must be known before a solution to the problem can be obtained. As a result, the approach presented here assumes that $\Phi^{l'l}$ is known.

When $\Phi^{l'l}$ is known, it is possible to approximate Eq. (37) using

$$\int_{4\pi} \Phi(\hat{s}', \hat{s}) d\Omega' \approx \sum_{l'=1}^{L} \Phi^{l'l} \Delta\Omega^{l'} \tag{39}$$

However, since $\Phi^{l'l}$ is the scattering from a discrete radiant direction $\hat{s}'$ into $\hat{s}$, the approximation will not satisfy Eq. (37) unless scattering is isotropic. As a result, phase function renormalization similar to the approach used in the DO method (Eq. 11) is required. An improved approach [20], which ensures the satisfaction of Eq. (37), is described next.

In this approach, the control angles $\Delta\Omega^{l'}$ and $\Delta\Omega^{l}$ are subdivided into smaller sub-control angles as shown in Fig. 9. The total energy scattered from $\Delta\Omega^{l'}$ into $\Delta\Omega^{l}$ is

$$\int_{\Delta\Omega^{l}} \int_{\Delta\Omega^{l'}} \Phi(\hat{s}', \hat{s}) d\Omega' d\Omega = \sum_{l_s=1}^{L_s} \sum_{l'_s=1}^{L'_s} \Phi^{l'_s l_s} \Delta\Omega^{l'_s} \Delta\Omega^{l_s} \tag{40}$$

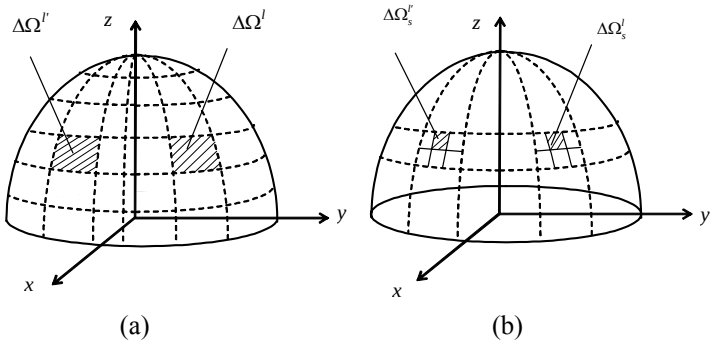

Figure 9 (a) Typical control angles, (b) possible sub-control angles.

where L'_s and L_s are the numbers of sub-control angles in $\Delta\Omega^{l'}$ and $\Delta\Omega^{l}$ respectively. For the example shown in Fig. 9b, $L'_s = L_s = 6$. The scattering phase functions $\Phi^{l'_s l_s}$ are evaluated along discrete radiant directions l'_s and l_s. The average scattering phase function is then calculated using

$$\overline{\Phi}^{l'l} = \frac{\int_{\Delta\Omega^{l}} \int_{\Delta\Omega^{l'}} \Phi(\hat{s}', \hat{s}) d\Omega' d\Omega}{\Delta\Omega^{l} \Delta\Omega^{l'}} = \frac{\sum_{l_s=1}^{L_s} \sum_{l'_s=1}^{L'_s} \Phi^{l'_s l_s} \Delta\Omega^{l'_s} \Delta\Omega^{l_s}}{\Delta\Omega^{l} \Delta\Omega^{l'}} \tag{41}$$

Using this approach, Eq. (37) is satisfied accurately.

5.5 Solution Procedure

The FV discretization results in a set of algebraic equations with the radiant intensities as the unknowns. Within each time step, an iterative method is used to solve the resulting set of equations. A marching order can be employed to efficiently solve the set of equations. For Cartesian grid problems, a possible marching order for a control angle pointing in the first quadrant is shown in Fig. 10. Extensions to the other three quadrants are straightforward and are left to the exploration of interested readers. The details of the program structure of using the FV method for solving the radiation heat transfer problems can be found in the user manual RAT [54]. The solution procedure for the situation depicted in Fig. 10 is summarized below for completeness.

1. Specify the initial intensity distribution for the whole domain.
2. Advance the time step to $t + \Delta t$.
3. Set the initial or the most current nodal intensities as the guessed values.
4. Update the "upstream" boundary intensities (left and bottom walls for the situation depicted in Fig. 10).
5. Following the marching order depicted in Fig. 10, calculate the nodal intensities for all internal control volumes.

6. Calculate the radiation arriving and leaving the right and top walls.
7. Return to step 4 and repeat the calculations until convergence.
8. Stop when the desired time is reached or go to step 2 to advance to a new time step.

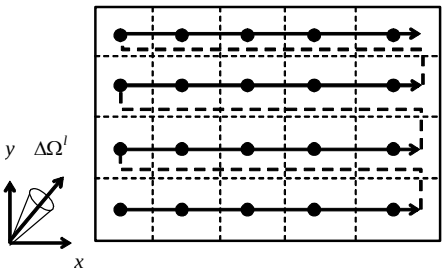

Figure 10 A possible marching order.

6 SPATIAL DIFFERENCING SCHEMES

The step scheme is used in the discretization equations presented in Section 5.3. The step scheme, although bounded, produces *false scattering* (see Section 8), which decreases the accuracy of the solution. Chai et al. [22] presented a study on spatial differencing schemes for radiation heat transfer. The study indicates that control volume boundary intensity should be calculated by tracing a beam to an appropriate "upstream" location where the intensity is known or can be approximated. The skewed "upwind" spatial differenting scheme (SUDS) of Raithby [5] is also used in radiation heat transfer problems which can be found in Chui and Raithby [18] and Chai et al. [20].

The step scheme produces reasonable solutions for steady-state problems. In transient problems, it fails to capture the penetration depth accurately during the initial transient [55, 57]. As a result, a bounded, high resolution scheme should be used. The $S^l_{c,HR}$ and $S^l_{p,HR}$ in Eqs. (36c) and (36d) are the additional sources due to high resolution schemes. Jessee and Fiveland [30] examined some high-resolution schemes for the DO method. The CLAM [4] scheme was recommended. Chai [55, 57] showed that the CLAM scheme captures the initial transient quite accurately. It should be pointed out that the additional source or sink terms for some high-resolution schemes can be negative. This can lead to negative intensities. Physically, radiant intensity is an always-positive variable. Therefore, negative intensity is physically unrealistic. The discretization equation should not allow the possibility of negative intensity as a solution. The always-positive variable treatment of Patankar [7] can be used to eliminate this possibility.

7 TREATMENT OF IRREGULAR GEOMETRIES

The procedure outlined above can be used to solve radiative transfer problems that can be described using Cartesian grids. Procedures for cylindrical geometries were reported by Moder et al. [25], Chui et al. [16], Kim and Baek [29] and Murthy and Mathur [34]. Irregular geometries can be handled using the blocked-off region procedure [23], spatial-multiblock procedure [27], body-fitted grids [18, 24, 32], and unstructured grids [33, 36, 41-44]. The blocked-off region procedure and spatial multiblock procedure are discussed below.

7.1 Blocked-Off Region Procedure

A simple procedure to model irregular geometries was presented by Chai et al. [23]. Only a brief description of the concept is presented here. Interested readers should refer to the above article. With this approach, the real domain shown in Fig. 11a is modeled using a nominal domain shown in Fig. 11b. The nominal domain is divided into two regions. These are (1) the *active* (unshaded) region, where solutions are sought, and (2) the *inactive* (shaded) region, which lies outside the real boundary; thus, solutions are not meaningful.

For irregular geometries with vertical or horizontal surfaces, the irregularities are captured exactly and no additional approximations are introduced by using the appraoch. Inclined and curved (Fig. 11c) boundaries can also be modeled using the proposed procedure. The inclined surfaces are however, approximated using staircase-like irregular geometries consist of vertical and horizontal surfaces. As a result, additional approximations are introduced in the modeling of inclined or curved surfaces.

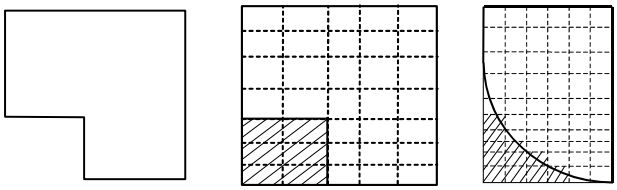

(a) (b) (c)

Figure 11 Irregular geometries: (a) real boundary condition, (b) simulated vertical and horizontal walls, and (c) simulated curved wall.

7.2 Spatial-Multiblock Procedure

The spatial-multiblock procedure divides the solution domain into a finite number of spatial blocks where spatial grids can be generated easily. Figures 12a and 12b show a situation where spatial-multiblock is beneficial. When body-fitted grids are used (Fig. 12a), significant changes in the aspect ratio of the grids are encountered in regions with large area variation. Figure 12b shows a spatial-multiblock grid. Fine grids can be embedded into selected region(s) as shown. Another possible benefit of spatial-multiblock lies in the fact that simpler spatial grids can be used to model complex geometries. The T-shaped enclosure shown in Fig. 12b is modeled using *Cartesian* grids. Figure 12c shows a situation where fine spatial grids are needed at one corner of the solution domain. When a single-block procedure is used, unnecessarily fine grids are also used in part of the remaining domain. A spatial-multiblock procedure can be used to eliminate this problem. Figure 12d shows a sample spatial-multiblock procedure for this problem. Fine grids are employed at the appropriate region of the domain. A method that ensures the conservation of radiant energy between blocks was presented by Chai and Moder [27].

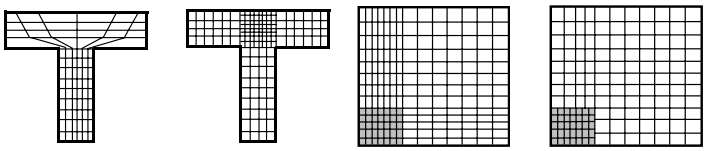

(a) (b) (c) (d)

Figure 12 Spatial grids: (a) single-block, (b) multiblock, (c) single-block, (d) multiblock.

8 RAY EFFECT AND FALSE SCATTERING

The FV method presented in this chapter, when used properly, is a flexible, efficient and accurate procedure for radiation heat transfer. However, similar to other numerical methods, the FV method for radiation heat transfer is not without shortcomings. If the FV method is to be used as the procedure of choice, it is important that these shortcomings are well understood. An in-depth discussion of two types of error, namely, the ray effect and the false scattering can be found in Chai et al. [19] and a possible remedy can be found in Li et al. [49].

9 REPRESENTATIVE WORKS

Significant advances in the modeling of radiative heat transfer have been reported using the DO and FV methods. Due to the volume of publication, a comprehensive review of the literature on these methods is not attempted. Selected publications are included here as a *starting* point for readers interested in further exploration. More complete collections of articles on the DO and FV methods can be found in Chai and Patankar [46], Siegel and Howell [48] and Modest [53]. The DO method has been used to model radiative transfer in Cartesian [9, 11, 12, 28, 38], cylindrical [8, 15, 17, 25], and irregular geometries [37, 39]. Truelove [11] presented ways to generate various moment-matching quadratures. Kim and Lee presented results for anisotropic scattering with collimated incidence [13]. The FV and DO methods were compared with the discrete transfer method by Coelho et al. [39]. Some representative articles on FV method can be found in Refs. [31, 35, 45]. Recently, the DO and FV methods have been used to study transient radiative transfer [40, 47, 50-52, 55-58].

10 CLOSING REMARKS

This article has described a numerical procedure for multidimensional radiative transfer process. Although most of the discussions are based on the FV method, major parts of this chapter are also valid for the DO method. This is due to the close similarity between the two methods. Both FV and DO methods have been thoroughly tested and widely used. The methods can provide accurate solutions for both steady-state and transient processes. Extensions to model non-gray radiation, non-diffuse walls and semitransparent media have also been reported.

11 REFERENCES

1. A. Schuster, Radiation Through a Foggy Atmosphere, Astrophysical Journal **21**, 1-22, 1905.
2. K. Schwarzschild, Uber das Gleichgewicht der Sonnenatmospharen, Akademie der Wissenschaften in Goettingen, Nachrichten. Mathematisch-Physikalische Klasse **1**, 41-53, 1906.
3. S. Chandrasekhar, Radiative Transfer, Dover Publications, Inc., New York, 1960.
4. B. Van Leer, Towards the Ultimate Conservative Difference Scheme. II. Monotonicity and Conservation Combined in a Second Order Scheme, Journal of Computational Physics **14**, 361-370, 1974.
5. G.D. Raithby, Skew Upstream Differencing Schemes for Problems Involving Fluid Flow, Computer Methods in Applied Mechanics and Engineering **9**, 153-164, 1976.
6. E.E. Khalil and J.S. Truelove, Calculation of Radiative Heat Transfer in a Large Gas Fired Furnace, Letters in Heat and Mass Transfer **4**, 353-365, 1977.
7. S.V. Patankar, Numerical Heat Transfer and Fluid Flow, Hemisphere Publishing Corp., Washington, D.C., 1980.
8. W.A. Fiveland, A Discrete Ordinates Method for Predicting Radiative Heat Transfer in Axisymmetric Enclosures, ASME Paper No. 82-HT-20, 1982.
9. W. A. Fiveland, Discrete Ordinates Solutions of the Radiative Transport Equation for Rectangular Enclosures, Journal of Heat Transfer **106**, 699-706, 1984.
10. W.A. Fiveland, Discrete Ordinates Methods for Radiative Heat Transfer in Isotropically and Anisotropically Scattering Media, Journal of Heat Transfer **109**, 809-812, 1987.
11. J.S. Truelove, Discrete-Ordinate Solutions of the Radiation Transport Equation, Journal of Heat Transfer **109**, 1048-1051, 1987.
12. A. S. Jamaluddin and P. J. Smith, Predicting radiative transfer in rectangular enclosures using the discrete ordinates method, Combustion Science and Technology **59**, 321-340, 1988.
13. T. K. Kim and H. S. Lee, Radiative Transfer in Two-Dimensional Anisotropic Scattering Media with Collimated Incidence, Journal of Quantitative Spectroscopy and Radiative Transfer **42** (3), 225-238, 1989.
14. G.D. Raithby and E.H. Chui, A Finite-Volume Method for Predicting a Radiant Heat Transfer Enclosures with Participating Media, Journal of Heat Transfer **112**, 415-423, 1990.
15. A. S. Jamaluddin and P. J. Smith, Discrete-Ordinates Solution of Radiative Transfer Equation in Nonaxisymmetric Cylindrical Enclosures, Journal of Thermophysics and Heat Transfer **6**, 242-245, 1992.
16. E.H. Chui *et al.*, Prediction of Radiative Transfer in Cylindrical Enclosures with the Finite Volume Method, Journal of Thermophysics and Heat Transfer **6**, 605-611, 1992.
17. S. Jendoubi *et al.*, Discrete Ordinates Solutions for Radiatively Participating Media in a Cylindrical Enclosure, Journal of Thermophysics and Heat Transfer **7**, 213-219, 1993.
18. E.H. Chui and G.D. Raithby, Computation of Radiant Heat Transfer on a Non-Orthogonal Mesh Using the Finite-Volume Method, Numerical Heat Transfer, Part B **23**, 269-288, 1993.
19. J.C. Chai *et al.*, Ray Effect and False Scattering in the Discrete Ordinates Method, Numerical Heat Transfer, Part B **24**, 373-389, 1993.
20. J.C. Chai *et al.*, Finite Volume Method for Radiation Heat Transfer, Journal of Thermophysics and Heat Transfer **8** (3), 419-425, 1994.
21. J.C. Chai et al., Improved Treatment of Scattering Using the Discrete Ordinates Method, Journal of Heat Transfer **116** (1), 260-263, 1994.
22. J.C. Chai *et al.*, Evaluation of Spatial Differencing Practices for the Discrete Ordinates Method, Journal of Thermophysics and Heat Transfer **8** (1), 140-144, 1994.
23. J.C. Chai *et al.*, Treatment of Irregular Geometries using a Cartesian Coordinates Finite-Volume Radiation Heat Transfer Procedure, Numerical Heat Transfer, Part B **26**, 225-235, 1994.
24. J.C. Chai *et al.*, Finite Volume Radiation Heat Transfer Procedure for Irregular Geometries, Journal of Thermophysics and Heat Transfer **9** (3), 410-415, 1995.
25. J.P. Moder *et al.*, Nonaxisymmetric Radiative Transfer in Cylindrical Enclosures, Numerical Heat Transfer, Part B **30**, 437-452, 1996.
26. J.P. Jessee and W.A. Fiveland, Bounded, high-resolution differencing schemes applied to the discrete ordinates method, Journal of Thermophysics and Heat Transfer **11**, 540-548, 1997.
27. J.C. Chai and J.P. Moder, Spatial-Multiblock Procedure for Radiation Heat Transfer, Numerical Heat Transfer, Part B **31**, 277-293, 1997.
28. M. A. Ramankutty and A. L. Crosbie, Modified Discrete Ordinates Solution of Radiative Transfer in Two Dimensional Rectangular Enclosures, Journal of Quantitative Spectroscopy and Radiative Transfer **57**, 107-140, 1997.
29. M.Y. Kim and S.W. Baek, Analysis of Radiative Transfer in Cylindrical Enclosures using the Finite Volume Method, Journal of Thermophysics and Heat Transfer **11** (2), 246-252, 1997.
30. J.P. Jessee and W.A. Fiveland, Bounded, High-Resolution Differencing Schemes Applied to the Discrete Ordinates Method, Journal of Thermophysics and Heat Transfer **11** (4), 540-548, 1997.
31. S.W. Baek, and M.Y. Kim, Analysis of Radiative Heating of a Rocket Plume Base with the Finite-Volume Method, International Journal of Heat and Mass Transfer **40** (7), 1501-1508, 1997.

32. J. Liu *et al.*, Prediction of Radiative Transfer in Genereal Body-Fitted Coordinates, Numerical Heat Transfer, Part B **31** (4), 423-439, 1997.
33. J.Y. Murthy and S.R. Mathur, Finite Volume Method for Radiation Heat Transfer Using Unstructured Meshes, Journal of Thermophysics and Heat Transfer **12** (3), 313-321, 1998.
34. J.Y. Murthy and S.R. Mathur, Radiative Heat Transfer in Axisymmetric Geometries using an Unstructured Finite-Volume Method, Numerical Heat Transfer, Part B **33**, 397-416, 1998.
35. S.W. Baek *et al.*, Nonorthogonal Finite-Volume Solutions of Radiative Heat Transfer in a Three-Dimensional Enclosure, Numerical Heat Transfer, Part B **34**, 419-437, 1998.
36. N. Vaidya, Multi-Dimensional Simulation of Radiation Using an Unstructured Finite Volume Method, AIAA paper 98-0856, 1998.
37. P. Sokolov, M. Ibrahim, and T. Kerslake, Computational Fluid Dynamics and Heat Transfer Modeling of Thermal Energy Storage Canisters for Space Applications, Presented at the 36th Aerospace Sciences Meeting & Exhibit, Jan 12-15, AIAA-98-1018, 1998.
38. M. A. Ramankutty and A. L. Crosbie, Modified Discrete Ordinates Solution of Radiative Transfer in Three Dimensional Rectangular Enclosures, International Journal of Heat and Mass Transfer **60**, 103-134, 1998.
39. P.J. Coelho *et al.*, Modelling of Radiative Heat Transfer in Enclosures with Obstacles, International Journal of Heat and Mass Transfer **41** (4-5), 745-756, 1998.
40. S. Kumar and K. Mitra, Microscale Aspects of Thermal Radiation Transport and Laser Applications, Advances in Heat Transfer **33**, 187-294, 1998.
41. J. Liu *et al.*, Development of an Unstructured Radiation Model Applicable for Two-Dimensional Planar, Axisymmetric, and Three-Dimensional Geometries, Presented at the 37th AIAA Aerospace Sciences Meeting & Exhibit, January 10 – 14, 1999, Reno, AIAA-99-0974.
42. N. Vaidya, An Unstructured Finite Volume Method for Nongray Radiation with Conjugate Heat Transfer and Chemistry, Presented at the 37th AIAA Aerospace Sciences Meeting & Exhibit, January 10-14, 1999, Reno, AIAA-99-0973.
43. J.C. Chai and J.P. Moder, Angular-Multiblock Procedure for Radiation Heat Transfer, Presented at the International Conference in Computational Heat and Mass Transfer, Gazimagusa, North Cyprus, 1999.
44. G.D. Raithby, Discussion of the Finite-Volume Method for Radiation, and its Application using 3D Unstructured Meshes, Numerical Heat Transfer, Part B **35**, 389-405, 1999.
45. S.R. Mathur, and J.Y. Murthy, Radiative Heat Transfer in Periodic Geometries using a Finite Volume Scheme, Journal of Heat Transfer **121**, 357-364, 1999.
46. J.C. Chai and S.V. Patankar, Finite-Volume Method for Radiation Heat Transfer, in W.J. Minkowycz and E.M. Sparrow (eds.), Advances in Numerical Heat Transfer **II**, Chap. 4, 109-138, Taylor & Francis, New York, 2000.
47. M. Sakami *et al.*, Transient Radiative Transfer in Anisotropically Scattering Media using Monotonicity-Preserving Schemes, Proceedings of IMECE 2000, November 5-10, 2000.
48. R. Siegel, and J.R. Howell, Thermal Radiation Heat Transfer, Taylor & Francis, New York, 2002.
49. H.S. Li *et al.*, Reduction of False Scattering of the Discrete Ordinates Method, Journal of Heat Transfer **124**, 837-844, 2002.
50. M. Sakami *et al.*, Analysis of Light-Pulse Transport Through Two-Dimensional Scattering and Absorbing Media, Journal of Quantitative Spectroscopy and Radiative Transfer **73**, 169-179, 2002.
51. M. Sakami *et al.*, Analysis of Short-Pulse Laser Photon Transport Through Tissues for Optical Tomography, Optics Letters **27** (5), 336-338, 2002.
52. Z. Guo, and S. Kumar, Discrete-Ordinates Solution of Short-Pulsed Laser Transport in Two-Dimensional Turbid Media, Applied Optics **40** (19), 3156-3163, 2002.
53. M.F. Modest, Radiative Heat Transfer, 2nd ed., Academic Press, New York, 2003.
54. J. C. Chai, A General Purpose Computer Program for Radiative Transfer– RAT, Version **1**, Radiative Heat Transfer by M. F. Modest, Second edition, 2003.
55. J.C. Chai, One-Dimensional Transient Radiation Heat Transfer Modeling using a Finite-Volume Method, Numerical Heat Transfer, Part B **44**, 187-208, 2003.
56. Z. Guo, and K. Kim, Ultrafast-Laser-Radiation transfer in Heterogeneous Tissues with the Discrete-Ordinates Method, Applied Optics **42** (16), 2897-2905, 2003.
57. J.C. Chai, Transient Radiative Transfer in Irregular Two-Dimensional Geometries, Journal of Quantitative Spectroscopy and Radiative Transfer **84**, 281-294, 2004.
58. I. Ayranci, and N. Selçuk, MOL solution of DOM for transient radiative transfer in 3-D scattering media, Journal of Quantitative Spectroscopy and Radiative Transfer **84** (4), 409-422, 2004.